Rapid Communications

Impact of asymmetries on fuel performance in inertial confinement fusion

M. Gatu Johnson,[1,*] B. D. Appelbe,[2] J. P. Chittenden,[2] J. Delettrez,[3] C. Forrest,[3] J. A. Frenje,[1] V. Yu. Glebov,[3] W. Grimble,[3] B. M. Haines,[4] I. Igumenshchev,[3] R. Janezic,[3] J. P. Knauer,[3] B. Lahmann,[1] F. J. Marshall,[3] T. Michel,[3] F. H. Séguin,[1] C. Stoeckl,[3] C. Walsh,[2] A. B. Zylstra,[4] and R. D. Petrasso[1]

[1]*Massachusetts Institute of Technology Plasma Science and Fusion Center, Cambridge, Massachusetts 02139, USA*
[2]*Centre for Inertial Fusion Studies, The Blackett Laboratory, Imperial College, London SW7 2AZ, United Kingdom*
[3]*Laboratory for Laser Energetics, University of Rochester, Rochester, New York 14623, USA*
[4]*Los Alamos National Laboratory, Los Alamos, New Mexico 87545, USA*

(Received 21 May 2018; revised manuscript received 20 July 2018; published 5 November 2018)

Low-mode asymmetries prevent effective compression, confinement, and heating of the fuel in inertial confinement fusion (ICF) implosions, and their control is essential to achieving ignition. Ion temperatures ($T_{\rm ion}$) in ICF experiments are inferred from the broadening of primary neutron spectra. Directional motion (flow) of the fuel at burn also impacts broadening and will lead to artificially inflated "$T_{\rm ion}$" values. Flow due to low-mode asymmetries is expected to give rise to line-of-sight variations in measured $T_{\rm ion}$. We report on intentionally asymmetrically driven experiments at the OMEGA laser facility designed to test the ability to accurately predict and measure line-of-sight differences in apparent $T_{\rm ion}$ due to low-mode asymmetry-seeded flows. Contrasted to CHIMERA and xRAGE simulations, the measurements demonstrate how all asymmetry seeds have to be considered to fully capture the flow field in an implosion. In particular, flow induced by the stalk that holds the target is found to interfere with the seeded asymmetry. A substantial stalk-seeded asymmetry in the areal density of the implosion is also observed.

DOI: 10.1103/PhysRevE.98.051201

Inertial confinement fusion (ICF) aims to achieve fusion burn by symmetrically compressing a spherical capsule filled with deuterium-tritium (DT) fuel to high convergence using lasers, either indirectly using a hohlraum [1] or with the laser beams directly incident on the target [2]. Independent of approach, control of low-mode asymmetries is of vital importance in the quest for ICF ignition [3–5]; such low-mode asymmetries have been identified as a primary performance-limiting factor for integrated national ignition facility (NIF) experiments [6]. Low-mode asymmetries will prevent effective compression and confinement of the fuel as well as effective conversion of shell kinetic energy to thermal energy of the fuel [7–9]. A consequence of low-mode asymmetries is residual kinetic energy of the fuel at burn (see, e.g., [3,6]). Accurate understanding of plasma ion temperature ($T_{\rm ion}$) from ICF implosions is important as $T_{\rm ion}$ is used as input for calculation of the pressure performance metric used to gauge progress towards ignition [10–12]. $T_{\rm ion}$ is traditionally inferred from the broadening of neutron spectra [13] and will thus also be sensitive to any residual fuel flows at burn, which will serve to artificially inflate the measured "$T_{\rm ion}$" [14–16] and, if the flows are asymmetric, lead to line-of-sight (LOS) variations in observed $T_{\rm ion}$. Such flow broadening has been invoked to explain discrepancies between measured and simulated $T_{\rm ion}$ for both indirect [17] and direct [18] drive implosions, but outstanding problems remain. As an example, minimal $T_{\rm ion}$ LOS variations have been observed in indirectly driven implosions at the NIF, while a large difference in measured deuterium-deuterium (DD) and DT $T_{\rm ion}$ indicates the presence of residual flows in these experiments [17]. In contrast, large $T_{\rm ion}$ LOS variations have been observed for directly driven implosions at OMEGA [18]. An improved understanding of the flow field in ICF implosions is essential both for assessing the impact of and learning how to mitigate low-mode asymmetries, and for interpretation of $T_{\rm ion}$ measurements.

In this Rapid Communication, we report on results from an experiment at the OMEGA laser facility [19] with intentionally imposed mode 2 asymmetries. The purpose of this experiment was to test the capability to accurately predict and measure the impact of a preimposed low-mode asymmetry on measured DT neutron spectra. Comparing $T_{\rm ion}$ asymmetry measurements from these perturbed implosions with three-dimensional (3D) simulations [20] not including the capsule stalk mount, we find that while the simulations partly capture the measurements, there is a clear remaining discrepancy. These $T_{\rm ion}$ asymmetry results in combination with x-ray self-emission imaging and measurements of areal density (ρR) asymmetries lead to the conclusion that the differences between measurements and simulations arise due to interplay between a stalk-seeded low-mode asymmetry and the imposed mode 2.

In the OMEGA experiment, five DT^{3}He-gas-filled, 870-μm outer-diameter plastic capsules with 14.5-μm-thick shells were imploded with all 60 available OMEGA laser beams (see Supplemental Material [21]). A 1-ns-duration laser pulse was used, with distributed phase plates and with two-dimensional smoothing by spectral dispersion [22] and polarization smoothing [23] applied. Total on-target illumination nonuniformity related to these factors <2% rms [24].

*Corresponding author: gatu@psfc.mit.edu

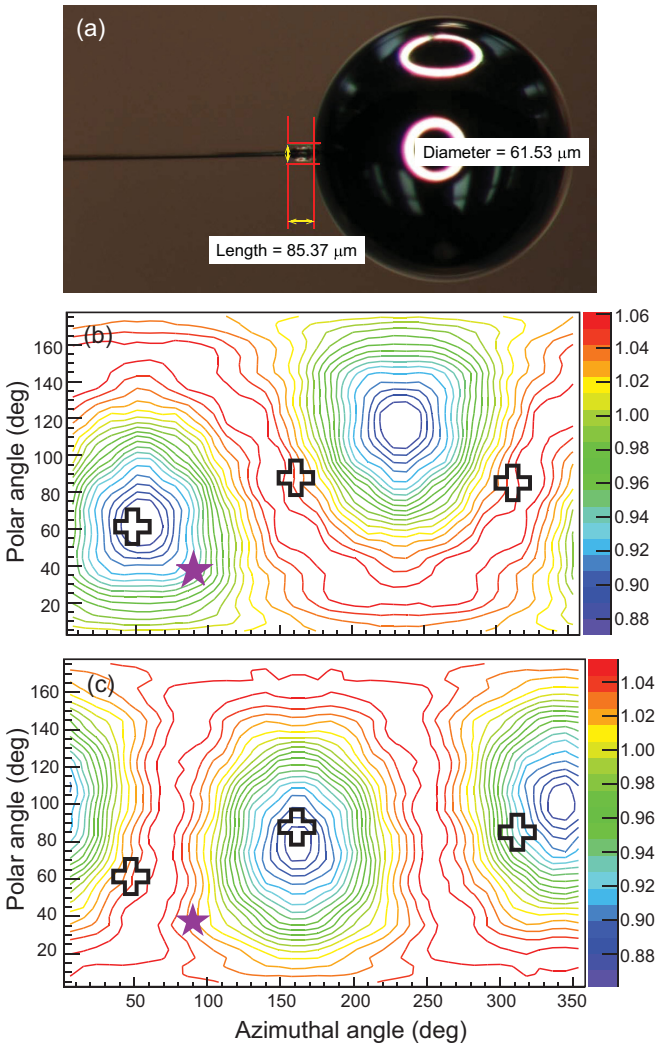

FIG. 1. (a) Picture of CH-shell capsule used in the OMEGA experiment mounted to the stalk with a glue spot with characterized length and diameter. (b) Asymmetry A and (c) Asymmetry B contour maps of laser intensity as a function of polar and azimuthal angle relative to the average laser intensity, illustrating the imposed mode 2. The plus signs represent the locations of the primary nTOF detectors; from left to right, 15.8 mntof, 12 mntof, and 5.0 mcvd. The purple star represents the location of the stalk.

Each capsule was held at the target chamber center (TCC) using a 17-μm-diameter SiC stalk attached with a glue spot [Fig. 1(a)]. One capsule was symmetrically imploded for reference with nominally 0.45 kJ laser energy per beam. Two mode 2 drive asymmetries with the same magnitude (19% peak to valley) but different orientation were designed for the remaining implosions by reducing the laser beam energy for 20–24 selected beams in two opposing cones around the implosion. These two asymmetries, henceforth denoted "Asym. A" [Fig. 1(b)] and "Asym. B" [Fig. 1(c)], were oriented to maximize the expected signatures in the three primary neutron spectrometer LOS [identified with black plus signs in Figs. 1(b) and 1(c)], and to "flip" the asymmetry between the two orientations. Two implosions of each asymmetry type were executed. The neutron spectra were measured using three neutron time-of-flight (nTOF) detectors: a scintillator-based detector 12 m from the implosion (12 mntof), a scintillator-based detector 15.8 m from the implosion (15.8 mntof), and a chemical vapor deposition (CVD)-diamond based detector 5 m from the implosion (5.0 mcvd) [25,26]. Implosion performance parameters are summarized in the Supplemental Material [21]. Measured $T_{\rm ion}$ ranged from 5.5 to 6.5 keV (including all LOS on all implosions). A DT neutron yield of 1.2×10^{13} was observed for the symmetric implosion, while an average yield of 7.4×10^{12} was obtained from the asymmetric implosions. This observed 36% yield reduction compares reasonably well to a 46% average reduction expected from 3D simulations. We note that the detrimental impact of low-mode asymmetries is expected to increase with implosion convergence [12], which explains why the yield reduction is not higher for these relatively low-convergence implosions.

The implosions were simulated postshot using the 3D CHIMERA code [20]. CHIMERA is initialized after the end of the laser pulse using output from one-dimensional (1D) HYADES [27] simulations, and run through convergence and disassembly. Previous work has shown that low-mode asymmetries can be expected to arise due to engineering features such as the stalk mount, fill tube, and/or support tent used to hold and fill an ICF target [28–32], due to unintended laser drive asymmetries [9,33,34], or due to unintentional capsule misalignment (offset) [35]. Capsule offsets are small for these room temperature implosions [36]; also see Supplemental Material [21]. The Chimera simulations, which use multigroup radiation transport, implement the measured laser beam energy balance [37,38] and are hence expected to capture effects due to laser drive asymmetry (this is done by initializing different regions around the implosion with HYADES simulations with varying drive). However, the simulations do not include the stalk mount. Synthetic neutron spectra are calculated for the three nTOF LOS [39] and simulated $T_{\rm ion}$ inferred from fits to the synthetic spectra.

Each nTOF provides a single neutron spectrum measurement integrated over burn, which means that the inferred $T_{\rm ion}$ is impacted by a burn-weighted averaging of the flow. The expected sign of the $T_{\rm ion}$ asymmetry depends sensitively on the timing of outflow along the asymmetry axis relative to burn. Early in the implosion, when the capsule is still compressing along all axes, maximum instantaneous $T_{\rm ion}$ is expected perpendicular to the asymmetry, while later in the implosion, after outflow starts along the axis of reduced laser energy, maximum $T_{\rm ion}$ is expected parallel to the asymmetry. According to the CHIMERA simulation, peak neutron production happens after the fuel has started moving outwards along the axis of the imposed mode 2 but while it is still moving inwards perpendicular to the asymmetry, which leads to maximum observed $T_{\rm ion}$ parallel to the asymmetry.

Measured and CHIMERA-simulated $T_{\rm ion}$ for the three nTOF LOS are contrasted in Fig. 2. Panel (a) shows the average difference in $T_{\rm ion}$ for each LOS between the symmetric reference and the two Asym. A implosions; panel (c) shows the same quantity for the two Asym. B implosions. (The symmetric reference is subtracted out to correct for any systematic differences between the three nTOF detectors.) The arrows below the plots indicate whether a detector is located parallel or perpendicular to the axis of the imposed mode 2 asymmetry.

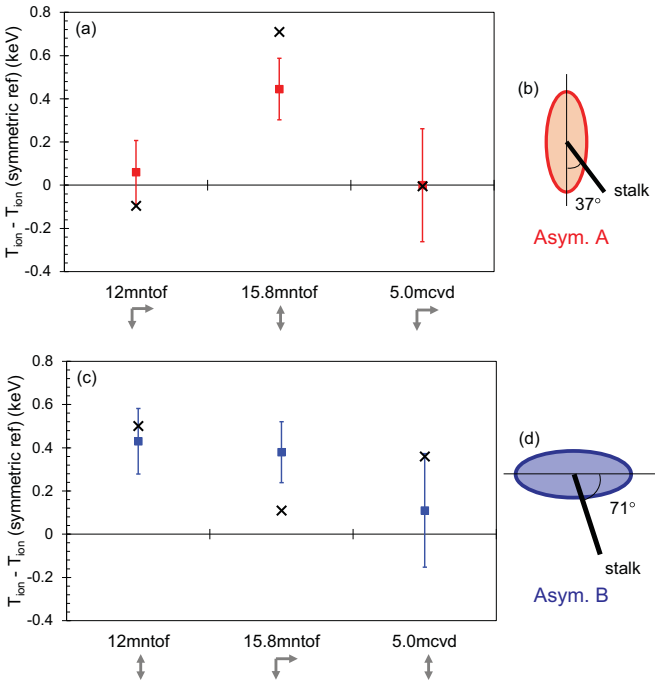

FIG. 2. Average T_{ion} for shots driven with (a) Asym. A and (c) Asym. B, minus T_{ion} for the symmetric reference shot. Points with error bars represent measured values in the three lines of sight using the 12 mntof, 15.8 mntof, and 5.0 mcvd detectors; black crosses 3D CHIMERA-simulated values for the same lines of sight. The gray arrows below the plots indicate whether a detector is located parallel or perpendicular to the axis of the imposed mode 2 asymmetry. Also shown are cartoons illustrating the angle between the imposed mode 2 and the stalk for the two drive configurations, Asym. A in (b) and Asym. B in (d); the thin black line represents the asymmetry axis.

For Asym. A [Fig. 2(a)], a clear enhancement in measured T_{ion} relative to the reference implosion is observed parallel to the imposed mode 2 (15.8 mntof), as expected from the CHIMERA simulations albeit slightly weaker than simulated. For Asym. B [Fig. 2(c)], the CHIMERA simulations also predict enhanced T_{ion} relative to the symmetric reference parallel to the imposed mode 2. In contrast, experimentally an overall enhancement in T_{ion} is observed in this case. The observed differences between measured and simulated results are believed to arise due to interplay between the imposed mode 2 and flow seeded by the capsule stalk mount, which is not included in the simulations. For Asym. A, the mode 2 is imposed at an angle of 37° from the stalk that holds the capsule [Fig. 2(b); in this illustration, the laser power is reduced at the tips of the ellipse and the thin black line represents the mode 2 axis]. We conjecture that the experimental effect on T_{ion} is smaller than simulated due to interference of stalk-seeded flow, which is not included in the simulation. For Asym. B, the mode 2 is imposed at a much larger angle to the stalk of 71° [Fig. 2(d)]. In this case, it appears as though the flows seeded by the mode 2 and the stalk counteract each other to eliminate LOS variations, while there is still clearly a substantial flow field induced in the implosion.

The hypothesis of asymmetry seed interplay is further supported by self-emission x-ray imaging of the converging implosions using an x-ray framing camera fielded at 79° from the imposed Asym. A and at 42° from the imposed Asym. B.

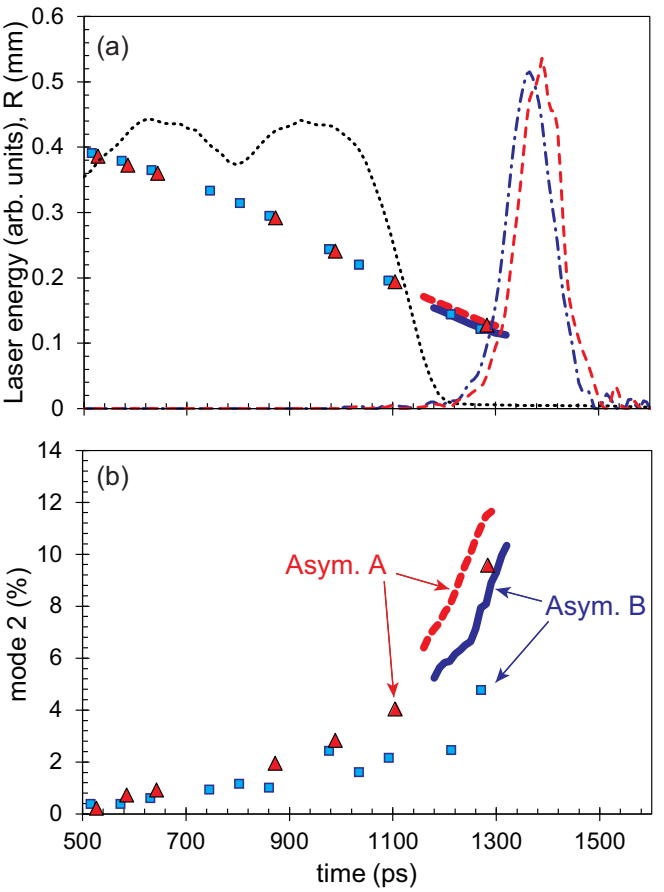

FIG. 3. (a) Measured shell trajectories as inferred from self-emission x-ray images for Asym. A (red triangles) and Asym. B (blue squares), contrasted to shell trajectories as inferred from CHIMERA-simulated x-ray images (thick red dashed and solid blue lines for the two cases). Also shown is the laser pulse shape (dotted black) and the burn history for the two implosions (red dashed line for Asym. A, broken blue line for Asym. B). (b) Mode 2 amplitude inferred from measured and simulated x-ray images, with the same color coding as in (a).

Shell radius and mode 2 as a function of time inferred from the measured x-ray images [40] are contrasted to CHIMERA simulations in Fig. 3. Because of the different fielding angle relative to the imposed mode 2, the x-ray images will see 98% of the asymmetry for Asym. A and 61% for Asym. B. (As the simulations consider the physical location of the x-ray framing camera, this is true both for experiments and simulation.) The implosion trajectory (radius vs time) is extremely well captured in the postshot simulations for both Asym. A and B [Fig. 3(a)], demonstrating that the simulations describe the overall implosion dynamics very well (note that simulated trajectories are only available at late time because of how CHIMERA is initialized). In contrast, the observed mode 2 [Fig. 3(b)] is significantly better captured for the Asym. A than for the Asym. B case. This again is consistent with an effect not included in the simulation (the stalk) substantially interfering with the imposed mode 2 for the Asym. B scenario.

Areal density asymmetry measurements for these implosions provide further evidence of the impact of the stalk. The experiment used a capsule fill gas composed of 38% D,

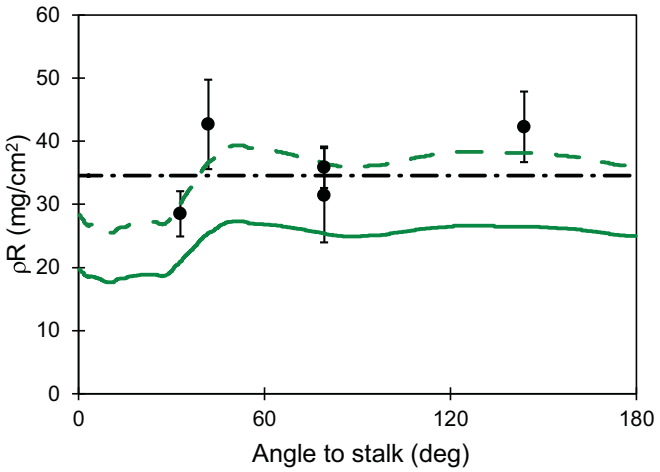

FIG. 4. Measured (points with error bars) and 2D-xRAGE-simulated (solid green line) ρR for the symmetric reference shot as a function of angle to the stalk. While the xRAGE simulation underestimates the overall ρR magnitude, it captures the shape of the asymmetry remarkably well: The dashed green line representing the xRAGE simulation renormalized to match the amplitude of the data matches the measurement with $\chi^2_{\text{red}} = 0.5$. In contrast, using a flat ρR (broken black curve) to describe the data gives $\chi^2_{\text{red}} = 1.6$.

38% T, and 24% ^{3}He, with ^{3}He included to allow for directional measurements of the D^{3}He proton spectrum. LOS variations in areal density were inferred based on D^{3}He proton energy downshifts observed using five different proton spectrometers distributed around the implosion [41]; also see Supplemental Material [21]. The results for the symmetric reference implosion are contrasted to two-dimensional (2D) xRAGE simulations [29,42] in Fig. 4. The xRAGE simulations include the stalk, but cannot simultaneously capture the impact of the stalk and the imposed mode 2 because of the 2D geometry. (This is why they are compared only to measurements from the symmetric reference implosion.) We find that while the average measured ρR (points with error bars in Fig. 4) is significantly higher than predicted by xRAGE (solid curve), the shape of the observed areal density variation is well captured by the simulation. If the amplitude of the xRAGE-simulated ρR curve is increased a factor of 1.44, an excellent description of the data is obtained (dashed curve, $\chi^2_{\text{red}} = 0.5$). For comparison, fitting a straight line ($\rho\text{R} = 34.6\,\text{mg/cm}^2$) to the data provides a much worse description (broken curve, $\chi^2_{\text{red}} = 1.6$). The data provide evidence that the weak spot in ρR around the stalk predicted by xRAGE is a real effect. We additionally note that while the implosions with imposed mode 2 show more variations in inferred ρR around the implosion than the symmetric reference as expected, all demonstrate the same weak spot at the location closest to the stalk (Supplemental Material [21]).

In summary, T_{ion} asymmetry measurements and x-ray self-emission imaging contrasted to 3D CHIMERA simulations both indicate a missing piece in the simulation, which based on the setup geometry is most likely flow induced by the stalk holding the capsule. ρR asymmetry measurements compared to 2D xRAGE simulations also indicate that the stalk introduces a substantial "weak spot" in the implosion, expected to be accompanied by an induced flow in the fuel. Together these observations lead to the conclusion that counteracting flows due to different asymmetry seeds must be considered when interpreting results from ICF implosions. When the various asymmetries directly counteract each other, as in Asym. B, an overall enhancement but small LOS variations in T_{ion} are observed. On the other hand, if asymmetry seeds align to reinforce each other, we can expect more significant LOS variations in T_{ion}. This type of argument likely explains the differences between T_{ion} observations for OMEGA and NIF cryogenically layered implosions discussed in the Introduction. At the NIF, we expect at minimum a mode 2 asymmetry in the drive due to the hohlraum geometry [33,34], a mode 4 asymmetry seeded by the capsule support tent [31,32,43], and a mode 1 asymmetry seeded by the fill tube [32]. Based on the results presented in this Rapid Communication, we hypothesize that the complex interactions of these modes lead to low LOS variations in T_{ion} but large overall flow broadening of the neutron spectra, consistent with NIF observations [17]. At OMEGA, on the other hand, we expect a mode 1 drive asymmetry [9], mode 1 introduced by unintentional capsule offsets [7], and mode 1 from the stalk; based on the present work, for shots where these various asymmetries align, we expect them to reinforce each other leading to large LOS variations in T_{ion}.

A couple of interesting additional observations can be made based on the present work. First, while there is no way of separating thermal from flow contributions to observed T_{ion} in the measurement, this is straightforward in the simulations. According to the CHIMERA simulations (Supplemental Material [21]), the minimum observed T_{ion} is 0.35 keV higher than thermal "no-flow" T_{ion} for the symmetric implosion, and 0.69–0.82 keV higher than no-flow T_{ion} for each of the asymmetrically driven implosions. This means that taking the minimum measured T_{ion} as a representation of thermal T_{ion} when calculating the pressure, as is currently often done for lack of a better method [12,44], is likely to significantly miss the mark. Second, the observed ρR asymmetry is an interesting result on its own. With an asymmetry this significant observed even for these relatively low-convergence implosions, significantly larger stalk-seeded ρR asymmetries can be expected to develop when the implosion is driven to converge more. Interestingly, recent efforts to predict performance of cryogenically layered implosions on OMEGA using data-driven statistical modeling suggest the presence of a persistent, systematic, but as of yet unidentified asymmetry seed in these implosions [45]; our results point to the target mount as the likely culprit.

Ultimately, a full understanding of the flow field in implosions and the impact of different asymmetry seeds is important in the efforts to control and minimize the imposed asymmetries, or maybe even exploit the flow field, as proposed in Ref. [46]. The results described in this Rapid Communication lay the groundwork for understanding the flow field in terms of asymmetry seed interplay, motivating further simulations and experiments to gain a broader understanding of the relationships.

In conclusion, T_{ion} and ρR asymmetry measurements and x-ray self-emission imaging from an experiment with imposed mode 2 asymmetries contrasted to simulations demonstrate

the impact of asymmetry seed interplay on the flow field in ICF implosions, and the impact of the capsule stalk mount on ρR asymmetries. The results represent a major step forward in the understanding of asymmetry seed impact on implosion dynamics, which is a complex problem that must be mastered to achieve ICF ignition.

The authors sincerely thank the OMEGA operations staff who supported this work, Bob Frankel and Ernie Doeg for processing the CR-39, and Michelle Evans for characterizing the target glue spots.

This material is based upon work supported by the Department of Energy, National Nuclear Security Administration, under Award No. DE-NA0002949, by the National Laser Users' Facility under Award No. DE-NA0002726, by LLE under Award No. 415935-G, and by Los Alamos National Laboratory operated by Los Alamos National Security, LLC, for the U.S. Department of Energy NNSA under Contract No. DE-AC52-06NA25396. This report was prepared as an account of work sponsored by an agency of the United States Government. Neither the United States Government nor any agency thereof, nor any of their employees, makes any warranty, express or implied, or assumes any legal liability or responsibility for the accuracy, completeness, or usefulness of any information, apparatus, product, or process disclosed, or represents that its use would not infringe privately owned rights. Reference herein to any specific commercial product, process, or service by trade name, trademark, manufacturer, or otherwise does not necessarily constitute or imply its endorsement, recommendation, or favoring by the United States Government or any agency thereof. The views and opinions of the authors expressed herein do not necessarily state or reflect those of the United States Government or any agency thereof.

[1] J. D. Lindl, P. Amendt, R. L. Berger, S. G. Glendinning, S. H. Glenzer, S. W. Haan, R. L. Kauffman, O. L. Landen, and L. J. Suter, Phys. Plasmas **11**, 339 (2004).

[2] R. S. Craxton *et al.*, Phys. Plasmas **22**, 110501 (2015).

[3] B. K. Spears, M. J. Edwards, S. Hatchett, J. Kilkenny, J. Knauer, A. Kritcher, J. Lindl, D. Munro, P. Patel, H. F. Robey, and R. P. J. Town, Phys. Plasmas **21**, 042702 (2014).

[4] C. Cerjan, P. T. Springer, and S. M. Sepke, Phys. Plasmas **20**, 056319 (2013).

[5] A. L. Kritcher *et al.*, Phys. Plasmas **21**, 042708 (2014).

[6] A. L. Kritcher *et al.*, Phys. Plasmas **23**, 052709 (2016).

[7] I. V. Igumenshchev *et al.*, Phys. Plasmas **23**, 052702 (2016).

[8] I. V. Igumenshchev *et al.*, Phys. Plasmas **24**, 056307 (2017).

[9] R. C. Shah, B. M. Haines, F. J. Wysocki, J. F. Benage, J. A. Fooks, V. Glebov, P. Hakel, M. Hoppe, I. V. Igumenshchev, G. Kagan, R. C. Mancini, F. J. Marshall, D. T. Michel, T. J. Murphy, M. E. Schoff, K. Silverstein, C. Stoeckl, and B. Yaakobi, Phys. Rev. Lett. **118**, 135001 (2017).

[10] R. Betti, P. Y. Chang, B. K. Spears, K. S. Anderson, J. Edwards, M. Fatenejad, J. D. Lindl, R. L. McCrory, R. Nora, and D. Shvarts, Phys. Plasmas **17**, 058102 (2010).

[11] R. Betti, A. R. Christopherson, B. K. Spears, R. Nora, A. Bose, J. Howard, K. M. Woo, M. J. Edwards, and J. Sanz, Phys. Rev. Lett. **114**, 255003 (2015).

[12] S. P. Regan *et al.*, Phys. Rev. Lett. **117**, 025001 (2016).

[13] L. Ballabio, J. Källne, and G. Gorini, Nucl. Fusion **38**, 1723 (1998).

[14] T. J. Murphy, Phys. Plasmas **21**, 072701 (2014).

[15] B. Appelbe and J. Chittenden, Plasma Phys. Controlled Fusion **53**, 045002 (2011).

[16] D. H. Munro, J. E. Field, R. Hatarik, J. L. Peterson, E. P. Hartouni, B. K. Spears, and J. D. Kilkenny, Phys. Plasmas **24**, 056301 (2017).

[17] M. Gatu Johnson *et al.*, Phys. Rev. E **94**, 021202(R) (2016).

[18] V. N. Goncharov *et al.*, Plasma Phys. Controlled Fusion **59**, 014008 (2017).

[19] T. R. Boehly, D. L. Brown, R. S. Craxton, R. L. Keck, J. P. Knauer, J. H. Kelly, T. J. Kessler, S. A. Kumpan, S. J. Loucks, S. A. Letzring, F. J. Marshall, R. L. McCrory, S. F. B. Morse, W. Seka, J. M. Soures, and C. P. Verdon, Opt. Commun. **133**, 495 (1997).

[20] J. P. Chittenden, B. D. Appelbe, F. Manke, K. McGlinchey, and N. P. L. Niasse, Phys. Plasmas **23**, 052708 (2016).

[21] See Supplemental Material at http://link.aps.org/supplemental/10.1103/PhysRevE.98.051201 for tables of target and laser parameters, implosion performance parameters, target offset measurements, inferred ρR values, and Chimera-simulated Tion values. Also included is a list of references describing the charged-particle spectrometers used to make the measurements from which ρR values are inferred.

[22] S. Skupsky, R. W. Short, T. Kessler, R. S. Craxton, S. Letzring, and J. M. Soures, J. Appl. Phys. **66**, 3456 (1989); S. P. Regan *et al.*, J. Opt. Soc. Am. B **22**, 998 (2005).

[23] T. R. Boehly, V. A. Smalyuk, D. D. Meyerhofer, J. P. Knauer, D. K. Bradley, R. S. Craxton, M. J. Guardalben, S. Skupsky, and T. J. Kessler, J. Appl. Phys. **85**, 3444 (1999).

[24] F. J. Marshall, J. A. Delettrez, R. Epstein, R. Forties, R. L. Keck, J. H. Kelly, P. W. McKenty, S. P. Regan, and L. J. Waxer, Phys. Plasmas **11**, 251 (2004).

[25] In ICF, the timescale for burn is short enough where the implosion time can be used as the start signal, and only a single detector is required for the nTOF measurement (the burn duration for these implosions is ~100 ps). Neglecting the impulse response of the detector, $E = 0.5md^2/t^2$, where m is the neutron mass, d detector distance, and t flight time.

[26] V. Yu. Glebov *et al.*, Rev. Sci. Instrum. **81**, 10D325 (2010); University of Rochester, Laboratory for Laser Energetics, National Laser Users' Facility Users Guide, http://www.lle.rochester.edu/media/about/documents/UsersGuide/05_UsersGuide.pdf (2014).

[27] J. T. Larsen and S. M. Lane, J. Quant. Spectrosc. Radiat. Transfer **51**, 179 (1994).

[28] I. V. Igumenshchev, F. J. Marshall, J. A. Marozas, V. A. Smalyuk, R. Epstein, V. N. Goncharov, T. J. B. Collins, T. C. Sangster, and S. Skupsky, Phys. Plasmas **16**, 082701 (2009).

[29] B. M. Haines *et al.*, Phys. Plasmas **23**, 072709 (2016).

[30] C. Stoeckl *et al.*, Phys. Plasmas **24**, 056304 (2017).

[31] R. Tommasini *et al.*, Phys. Plasmas **22**, 056315 (2015).
[32] C. R. Weber *et al.*, Phys. Plasmas **24**, 056302 (2017).
[33] A. Pak *et al.*, Phys. Plasmas **24**, 056306 (2017).
[34] L. Divol *et al.*, Phys. Plasmas **24**, 056309 (2017).
[35] J. R. Rygg, J. A. Frenje, C. K. Li, F. H. Séguin, R. D. Petrasso, F. J. Marshall, J. A. Delettrez, J. P. Knauer, D. D. Meyerhofer, and C. Stoeckl, Phys. Plasmas **15**, 034505 (2008).
[36] Offsets of 8–16 μm were measured using x-ray pinhole imaging for these implosions.
[37] W. R. Donaldson, J. Katz, R. Huff, E. M. Hill, J. H. Kelly, J. Kwiatkowski, R. B. Brannon, and R. Boni, Rev. Sci. Instrum. **87**, 053511 (2016).
[38] The beam energy balance is measured prior to entry into the target chamber and must be corrected for transmission through the final optics and blast shields, which can introduce large uncertainties. The implosions described here were taken the day after blast shield replacements, which means the beam energy balance measurements are expected to be accurate.
[39] B. Appelbe and J. Chittenden, High Energy Density Phys. **11**, 30 (2014).
[40] D. T. Michel *et al.*, High Power Laser Sci. Eng. **3**, e19 (2015).
[41] Wedge range filter (WRF) proton spectrometers, charged particle spectrometers (CPS), and the magnetic recoil spectrometer (MRS) were used for these measurements.
[42] M. Gittings, R. Weaver, M. Clover, T. Betlach, N. Byrne, R. Coker, E. Dendy, R. Hueckstaedt, K. New, W. R. Oakes, D. Ranta, and R. Stefan, Comput. Sci. Discovery **1**, 015005 (2008); C. H. Aldrich, J. M. Campbell, R. M. Rauenzahn, and C. A. Wingate, Phys. Plasmas **24**, 052701 (2017).
[43] R. H. H. Scott, D. S. Clark, D. K. Bradley, D. A. Callahan, M. J. Edwards, S. W. Haan, O. S. Jones, B. K. Spears, M. M. Marinak, R. P. J. Town, P. A. Norreys, and L. J. Suter, Phys. Rev. Lett. **110**, 075001 (2013).
[44] O. A. Hurricane *et al.*, Nature **506**, 343 (2014).
[45] V. Gopalaswamy *et al.*, Tripling the Fusion Yield in Direct-Drive Laser Fusion through Predictive Statistical Modeling (unpublished).
[46] J. L. Peterson, K. D. Humbird, J. E. Field, S. T. Brandon, S. H. Langer, R. C. Nora, B. K. Spears, and P. T. Springer, Phys. Plasmas **24**, 032702 (2017).